Heliyon 9 (2023) e18857

Contents lists available at ScienceDirect

Heliyon

journal homepage: www.cell.com/heliyon

Formation of an unprecedented yellow snow episode in Xinjiang on December 1, 2018

Haibo Huang [a,*], Yu Wan [b]

[a] Meteorological Center of Xinjiang Air Traffic Management Bureau, Urumqi, Xinjiang, China
[b] Xinjiang Meteorological Observatory, Urumqi, Xinjiang, China

ARTICLE INFO

Keywords:
Yellow snow
Dust
HYSPLIT model
MERRA-2
ECMWF model

ABSTRACT

On 1 December 2018, a heavy yellow snow fell in Urumqi (87°37′E, 43°47′N) — the largest city of northwest China's Xinjiang province, which was the first case that the yellow snow has been observed in winter. The air parcel trajectories obtained from Hybrid Single-Particle Lagrangian Integrated Trajectory (HYSPLIT) model and the dust surface mass concentration from Modern-Era Retrospective Analysis for Research and Applications Version 2 (MERRA-2) were adopted to identify the potential sources and transport paths of pollutants responsible for this yellow snow episode. The meteorological situation and the European Center for Medium-Range Weather Forecasts (ECMWF) forecast products have been utilized to analyze the supportive meteorological conditions. The results showed that the heavy snow in Urumqi was contaminated by the yellow dust originated in Karamay of Xinjiang province. The strong surface winds in Karamay lifted large amounts of dust into the atmosphere. Then the airborne dusts were transported to Urumqi rapidly by strong low-level winds, where precipitation in connection with the upper trough and the cold front lead to the yellow snow episode. This study can provide important scientific significance for predicting this kind of event (yellow snow).

1. Introduction

Snow in its purest form is white, but other colors of snow exist, including yellow [1,2], brown [3,4] and even red [5,6]. The coloured snow is usually associated with pollen, spores, algae, mineral dust or coloured soil particles transported by the air [3,5–13].

Yellow snow often causes concern because they may come from industrial waste, chemical elements or radioactive fallout with hazardous materials and therefore pose health risks to human beings [14]. Only few episodes of this kind have been documented and studied in Europe and northern part of European Russia. Among them, Franzén et al. [1,2] analyzed a yellow snow episode of northern Fennoscandia on 10 March 1991. The results showed that the dust originated in the Sahara desert and the precipitation in connection with the arctic front caused the yellow snow, rather than an influx of pollutants from industrial smoke, as reported by the local weather service. Shevchenko et al. [8] investigated snow samples from five points in study area, and concluded that the yellow snow event in Northern European Russia in March 2008 was the result of the mineral dust falling on the snow. The main source of dust responsible for the yellow color of snow is semi-desert and steppe regions of Northwest Kazakhstan. In China, yellow snow has occasionally been observed in spring. One recent example of such a phenomenon occurred in April of 2015 when snow fell with a yellow tint (http://www.weather.com.cn/xinjiang/xjsy/tqyw/2987110.shtml).

* Corresponding author.
E-mail address: hhb-0820@163.com (H. Huang).

https://doi.org/10.1016/j.heliyon.2023.e18857
Received 2 March 2023; Received in revised form 27 July 2023; Accepted 31 July 2023
Available online 1 August 2023

The purpose of this study was to investigate an unprecedented yellow snow episode. Yellow snow in winter around the world has not been found in published papers so far. Such a shortage of knowledge about yellow snow represents a major uncertainty in the ability of forecasters to predict similar event. The episode described in this article was the first case that the yellow snow has been observed in winter. This study mainly investigated the characteristics of this event in three aspects: (1) why the snow was coloured in yellow, (2) where the pollutants came from, (3) how the pollutants reached the target location.

2. Data and methods

2.1. Study area

Located upwind of Xinjiang province, Kazakhstan is the world's largest landlocked country characterized by sharply continental climate, hot summers alternating with cold winters, especially in the plains and valleys [15]. It stretches from Central Asia to Eastern Europe, bounded on the east by China nearly one-third of the country's area is the Kazakh Steppe. Xinjiang province is the China's largest administrative region at the provincial level with a large area spanning over 1.6 million km^2, which covers one sixth of the country's territory. However, only about 4.3% of its land is habitable. The rest is mostly desert such as Gobi, snow-capped mountains and glaciers. It borders East Kazakhstan(Fig. 1). Urumqi (87°37′E，43°47′N) is in the north part of Xinjiang province and is characterized by a temperate continental arid climate [16]. Urumqi International Airport (87°28′E, 43°54′N) is about 17 km northwest of Urumqi city. Karamay (84°51′E，45°37′N) is an important precursor station to major weather events occurred in Urumqi and lies in northwest of Xinjiang province, 310 km upstream of Urumqi. It is surrounded by the Gobi Desert and is characterized by a continental arid-desert climate [17].

2.2. HYSPLIT model

The HYSPLIT model from NOAA is one of the most extensively used atmospheric transport and dispersion models to compute air parcel trajectories, as well as complex transport, dispersion, chemical transformation, and deposition simulations [18–29].

In order to identify potential sources and transmission paths of pollutants responsible for the yellow snow episode, the National Oceanic and Atmospheric Administration (NOAA) HYSPLIT model online with the 1° × 1° data of global data assimilation system (GDAS1), which is provided by National Centers for Environmental Prediction (NCEP), were run to get backward and forward trajectories of air parcels at different heights (500 m, 1000 m and 1500 m) above the ground level (AGL).

Fig. 1. Map of the study area.

The trajectory heights were set to 500 m, 1000 m and 1500 m AGL, because the winds at these heights can effectively reduce the influence of ground surface friction and more accurately reflect the characteristic of the mean flow field in the atmospheric boundary layer according to previous studies [23,30–32]. Two other mainoptions applied in this paper are Vertical Motion/Model vertical velocity and Plot projection/Lambert.

2.3. MERRA-2 analysis

The Modern-Era Retrospective Analysis for Research and Applications, version 2 (MERRA-2) improved the successful original MERRA reanalysis with an approximate resolution of $0.5^\circ \times 0.625^\circ$ and 72 hybrid-eta levels from the surface to 0.01 hPa, updated every 6 h [33]. It is intended as an intermediate reanalysis and includes aerosol data assimilation, so it can provide a multidecadal reanalysis in which aerosol and meteorological observations are jointly assimilated within a global data assimilation system [34].

The MERRA-2 analysis was performed to investigate the selected case study in more detail. We used a domain between 43.5°–52.5°N/75°–95°E for the study area. Hourly surface concentration field of dust (M2T1NXAER V5.12.4), estimated by Modern-Era Retrospective Analysis (collection version 5.2.0) for Research and Applications Version 2 (MERRA-2) [34,35] were adopted in this study to confirm the deposition of pollutants (dusts) in the areas mapped by our study. The MERRA-2 data can be obtained through the platform "Giovanni" (https://giovanni.gsfc.nasa.gov/giovanni), which was developed and maintained by the National Aeronautics and Space Administration (NASA) Goddard Earth Science Data and Information Services Center [36].

2.4. Meteorological data

Synoptic weather systems and strong winds associated with cold-frontal passages are the primary drivers of global dust emissions and transport [37]. Both surface weather charts and upper weather charts along with observations of meteorological stations from the Chinese Meteorological Administration (CMA) were used to analyze the supportive meteorological conditions that led to the strong winds capable of generating and transporting the pollutants (dusts). The temporal resolutions of surface weather chart and upper weather charts are 3 h and 12 h respectively.

2.5. ECMWF forecasts

The Medium-Range Weather Forecasts (ECMWF) products have been widely used by regional operational forecast centers in China. Some evaluation studies on regional forecasts in China showed that the forecast accuracy of ECMWF model is higher than those of the other forecast centers [38,39]. Since the temporal resolution of upper observations is always very low (12 h), the ECMWF products initiated at 08:00 Local Standard Time (referred to as LST hereon, LST = UTC + 8 h) on 30 November 2018 for futute 36 h at 3-h intervals with the spatial resolution of $0.25^\circ \times 0.25^\circ$ were used to display more details of surpportive meteorological elements.

Fig. 2. An airplane polluted by the yellow snow was waiting for cleaning at Urumqi International Airport on December 1, 2018.

3. Results and discussions

3.1. Description of the episode

On 1 December 2018, a heavy snow reached Urumqi and its surrounding areas. Urumqi was most heavily affected with the largest snowfall amount of 16.6 mm. The snowfall started at 06:00 LST early in the morning and stopped at 17:00 LST in the afternoon. After sunrise, it was found that the snow appeared with a yellowish color (Fig. 2). Before the event, the heavy snow was anticipated in Urumqi, but not the yellow snow. It seriously polluted the local air. No alarming and recommending precautions for sensitive populations had been released prior to the event reaching Urumqi. Consequently, this unprecedented yellow snow made thousands of people outside choking on such a heavily polluted day. Many worried people phoned local meteorological authorities to ask why did the snow turn yellow and whether the snow was contaminated by industrial waste or chemical elements.

A preliminary analysis, based on visual observations at the site and on the sample analysis, allowed the identification of yellow pollutants. Specifically, a qualitative yellow snow sample was collected with an iron vessel from the upper part of the snow cover, where the yellow pollutants had sunk to a depth of a few centimetres. The sample was melted and dried. It was found that the yellowish, dried remains inside the vessel consisted of small aggregates of mineral material (dust), similar to that of the upper parts of the soil, which tainted the snow yellow and heavily polluted the air. That is to say, the dust was responsible for the yellow snow, not the industrial waste or chemical elements. Dust event was very scarce in winter and they usually occurred in the spring and early summer months in China [40,41]. During the event, hourly visibility of 200 m was reported in several parts of the city, which resulted in many car accidents. The Urumqi International Airport was forced to close because of the heavy snow mixed with a large quantity of dust. Nearly 450 flights were canceled, delayed or diverted and more than 4000 passengers were stranded in terminal halls.

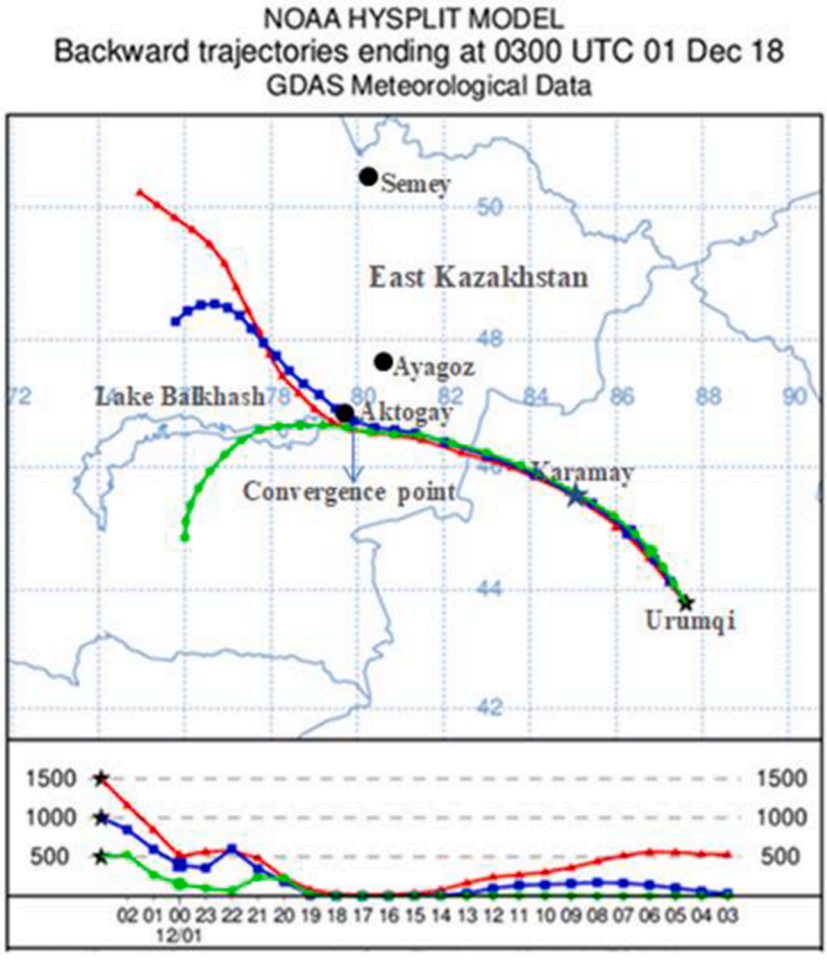

Fig. 3. Calculated backward trajectories of air parcels at 1-h intervals for the 24-h period ending at 11:00 LST 1 December 2018 originating from Urumqi at the heights of 500 m, 1000 m and 1500 m above the ground level (AGL). Top portion shows the horizontal path, and the bottom portion shows the vertical path of the trajectories.

3.2. Dust source identification

Another important issue to investigate is where the dust came from. The HYSPLIT model is one of the most widely used methods for studying dust storms [42–44]. In this work, GDAS1 1° × 1° data were provided as input to the HYSPLIT model for computing back and forward trajectories for source identification. MERRA-2 reanalysis data have been utilized to confirm the deposition area of dust particles.

3.2.1. Air parcel trajectories

For the present study, backward trajectories of air parcels ending at the time of the yellow snow observation at Urumqi, back to their origins 24 h earlier, were calculated. It seemed that the trajectories from different heights converged at a point (46°75′N, 80°00′E) near Aktogay in Kazakhstan, and then moved southeasterly to Xinjiang Province, passed through Karamay and reached Urumqi at 03:00 LST on December 1, 2018 (Fig. 3). Did the dust responsible for the yellow snow in Urumqi come from Kazakhstan?

Different methods have been used to identify and characterize dust sources [45]. The backward trajectory analysis is a useful tool for dust source identification, but it has some limitations. For example, it may overestimate the impact of less polluted areas where a trajectory event was observed [46] or misrepresent the turbulent mixing processes that air parcels experience during transport [47,48]. Comprehensive analysis of backward and forward air parcel trajectories may produce a more realistic depiction of the link between Urumqi and the dust sources.

Based on the above considerations, the forward trajectories of air parcels in future 24 h starting from two potential dust source, the convergence point in Kazakhstan at 11:00 LST on November 30, and Karamay at 03:00 LST on 1 December 2018, were calculated respectively, to check whether the dust paricles walked on their way to Urumqi.

The forward trajectories moving from the convergence point in Kazakhstan revealed that the dust dispersion directions at the different heights (2000–4000 m AGL) were all to the northeast (Fig. 4a), under the prevailing upper wind flow of southwesterly relative to the observation sites, as it will be discussed later in next section, far away from Karamay and Urumqi. It is unlikely that the dust source in Kazakhstan has relations with the yellow snow in Urumqi.

For trajectories starting from Karamay, air parcels at the different heights went straight to Urumqi, although they went their separate ways when they left Urumqi (Fig. 4b). Specifically, the air parcels near the ground at 500 m AGL moved to southern part of Xinjiang Province, but the air parcels at higher levels (1000 m and 1500 m AGL) spreaded to Mongolia and Siberia, similar to those forward trajectories starting from the convergence point in Kazakhstan.

3.2.2. Dust surface mass concentration

Fig. 5 shows the spatial distribution of dust surface mass concentration from 23:00 LST on 30 November 2018 to 23:00 LST 1 on December 2018. There was just one isolate dust region with low concentration near Lake Balkhash, about 600 km away from Karamay and 900 km from Urumqi. The maximum of dust surface mass concentration was in Karamay. From Karamay to Urumqi, the dust concentration decreased gradually.

From the dust concentration map, it can be inferred that the dust responsible for the yellow snow in Urumqi came from the dust emission process in Karamay and its surrounding areas on 1 December 2018, and the dust source areas in Kazakhstan have not contributed to the dust transported towards Urumqi.

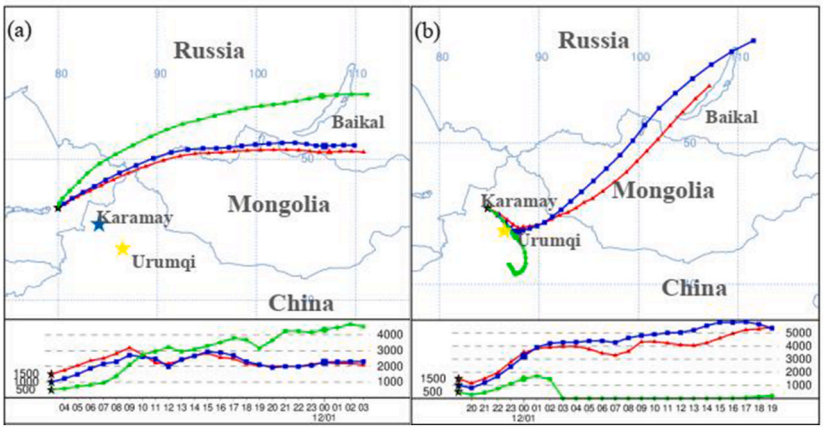

Fig. 4. Calculated forward trajectories of air parcels at 1-h intervals for the 24-h period starting from convergence point (**a**) at 11:00 LST on 30 November 2018, (**b**) from Karamay at 03:00 LST on 1 December 2018 at the heights of 500 m, 1000 m and 1500 m above the ground level (AGL). Top portion shows the horizontal path, and the bottom portion shows the vertical path of the trajectories.

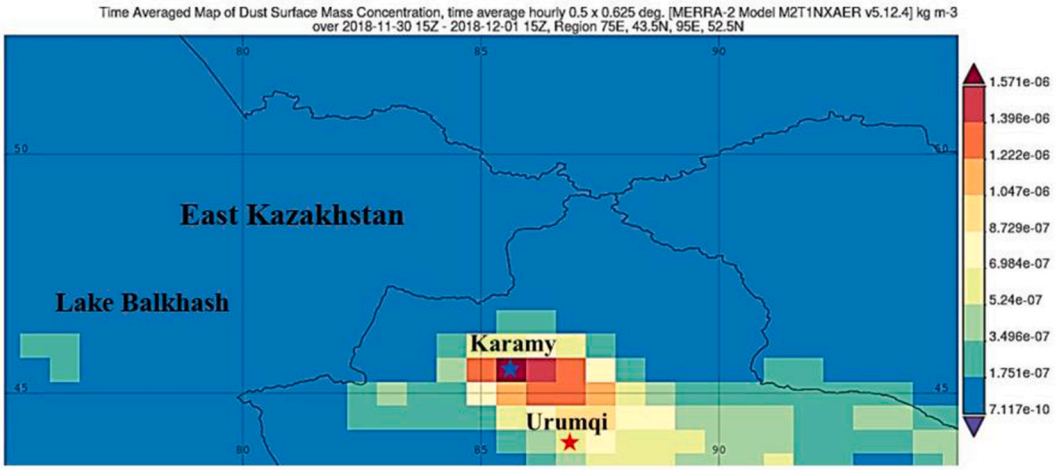

Fig. 5. Spatial distribution of dust surface mass concentration from 23:00 LST on 30 November 2018 to 23:00 LST on 1 December 2018 obtained from MERRA-2.

3.3. The meteorological analysis

3.3.1. Surface observations

Fig. 6 showed surface observations of meteorological stations in Kazakhstan, China, Siberia and Mongolia on 30 November and 1 December 2018. The solid (dashed) yellow circles indicate the weather stations with dust storm (dust) observations. There was only one station in Kazakhstan at which dust storm was reported and there was no dust distribution in China at 08:00 LST on 30 November (Fig. 6a). More dust storm observations were found in parts of Kazakhstan and Siberia at 20:00 LST on 30 November, but loosely distributed (Fig. 6b). The dust storm observations outside China had a tendency to move east and became more loosely at 08:00 LST on 1 December. There was no obvious dust distribution in China besides Karamay at that time (Fig. 6c). Discrete dust storm observations were reported in Kazakhstan, Mongolia and in the east side of the Baikal at 20:00 LST on 1 December. However, the dust or dust storm observations downwind of Karamay in China increased rapidly (Fig. 6d) and they coincided with the spatial distribution of dust surface mass concentration presented in Fig. 5. The stations in Mongolia and Siberia, where dust were observed, are basically in the path of the

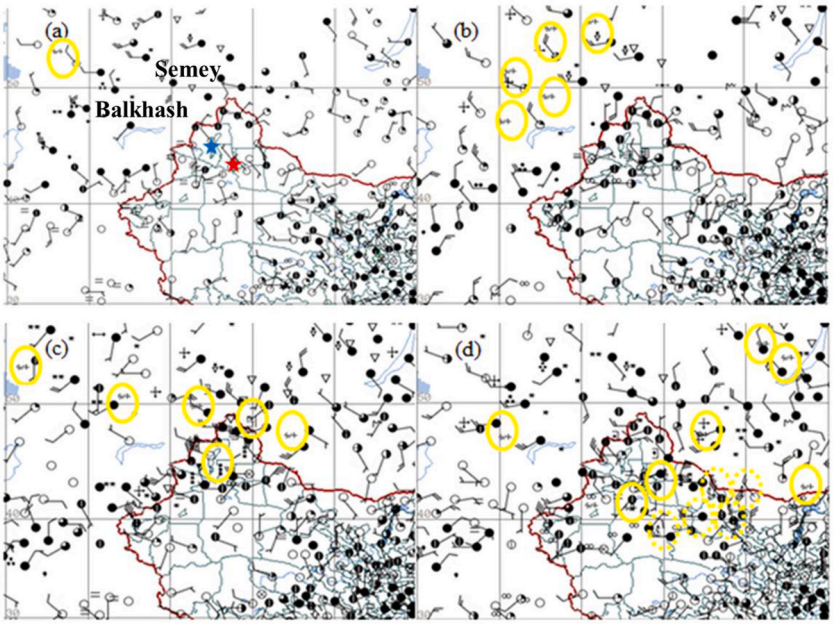

Fig. 6. Surface observations at (**a**) 08:00 LST, (**b**) 20:00 LST on 30 November 2018, and (**c**) 08:00 LST and (**d**) 20:00 LST on 1 December 2018. The symbol (●) denotes the weather station position. The solid (dashed) yellow circle indicates the weather stations where dust storm (dust) was reported.

forward trajectories starting from the convergence point in Kazakhstan and Karamay in China at higher levels. It proved that the dust forward trajectories calculated from HYSPLIT model were reasonable.

Wind affects tremendously both the dust emission and the dust transport [49]. On the surface wind field presented in Fig. 6, it was obvious that only the dust regions with northwesterly wind in Kazakhstan and Karamay had the potential to transport the dust to Urumqi. However, the wind speeds of these stations in Kazakhstan were 4–8 m s^{-1}, it meant that the dust particles originated from the nearest station in Kazakhstan would take about 20–40 h to reach Karamay and about 30–60 h to reach Urumqi. At this rate, the dust particles were likely to reach Karamay at 16:00 LST on 1 December and Urumqi at 06:00 on 2 December at the earliest, much later than the occurrence time of dust in Karamay and Urumqi. According to the analysis of air parcel trajectories, spatial distribution of dust surface mass concentration and surface observations, the dust source areas located in Kazakhstan have not contributed to the dust invaded Urumqi.

3.3.2. *Atmospheric circulation*

One day before the yellow snow episode, an upper trough moved quickly eastward (Fig. 7a). Ahead of the trough, the Central Asia and northern parts of Xinjiang Province were dominated by the strong southwesterly winds, providing generation and maintenance of unstable atmospheric conditions favorable for the precipitation and strong winds [50]. The atmospheric circulation at the mean sea level over Xinjiang Province was characterized by a large, quasi-stationary anticyclone centered on Mongolia (Fig. 7b). On its northwestern side, a Siberian frontal cyclone (low pressure) was moving easterly, drived by a cold high pressure system. The frontal cyclone was sandwiched by a slow moving anticyclone ahead and a strong anticyclone developing behind when it moved close to Xinjiang Province. It rapidly intensified the pressure gradient, resulting in postfrontal strong winds, especially in Karamay region.

Before the arrival of the cold front, the weather in Karamay was relatively calm; the air temperature was ~4 °C, the sea level pressure had dropped to its minimum, and the surface wind was relatively light with the wind direction ranging from 160° to 180° (southerly). In the early morning of December 1, the wind swung to a northerly direction and wind speed rapidly increased to 23 m s^{-1} with a maximum gust speed of 32 m s^{-1}. Fig. 8a presents time series of wind speeds and visibilities in Karamay. This record-breaking strong wind in winter since 1971 battered Karamay and triggered severe dust storm, which lasted about 13 h with visibilities ranging from 100 to 800 m. The dust particles were lifted from the ground level by surface strong winds under the influence of the cold front with the unstable atmosphere layer associated with the upper trough, which is common in spring and early summer but rarely in winter [50]. As the upper trough and cold front moved eastward, a large quantities of dust swept across parts of northern Xinjiang from west to east and polluted Urumqi (Fig. 8b).

3.3.3. *Vertical profile*

For the present study, the ECMWF model predicted in advance the atmospheric circulation, the strong wind episode in Karamay and the heavy snow in Urumqi of timing and magnitude that compared reasonably well with the observations. Fig. 9 shows the time series of vertical structure of wind, temperature and high Relative Humidity (RH) area over Karamay derived from ECMWF forecasts initiated at 08:00 LST on 30 November 2018. As well known, sudden changes in temperature have significant influences on the wind speed and direction, and the high RH area (RH $\geq$ 70%) extended to the ground is always associated with the precipitation when an upper trough and/or a cold front is approaching.

Our focus is on the wind fields above the ground because they determine whether the dust, lifted by the surface strong wind, can be transported far away. The winds at all levels over Karamay increased rapidly from 02:00 LST on 30 November when the upper trough and surface cold front were approaching, especially low-level (925 hPa and 850 hPa) winds, which were much stronger than surface winds. Remarkably, the direction of low-level wind turned to northwesterly from then on, which was favorable for blowing dust to Urumqi. While the wind directions of middle-level (700 hPa) and upper-level (500 hPa and above) wind direction were southwesterly

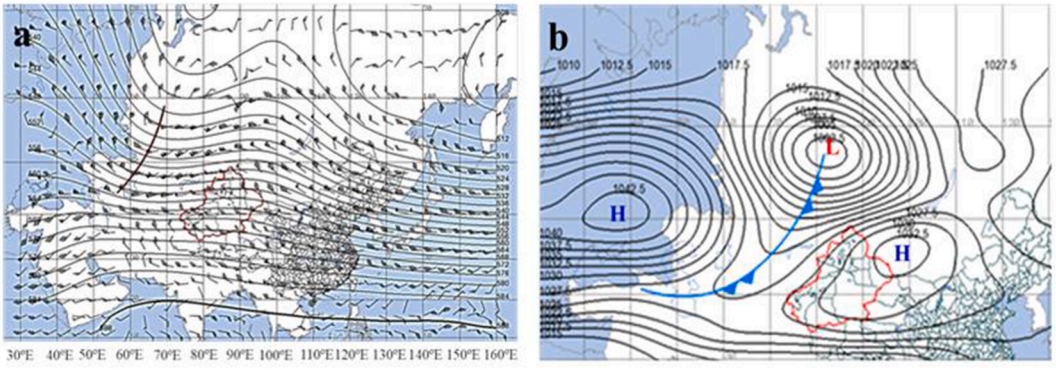

Fig. 7. Weather charts at 08:00 LST on 30 November 2018 obtained from the CMA. (**a**) Observations of 500 hPa winds (a full barb denotes 4 m s^{-1} and a black pennant denotes 20 m s^{-1}), geopotential heights (solid, every 4 dagpm); (**b**) Sea Level Pressure (solid, every 2.5 hPa). The brown curve stands for the upper trough and the blue curve for cold front. The symbol "H" represents high pressure (anticyclone) while the symbol "L" denotes low pressure (cyclone).

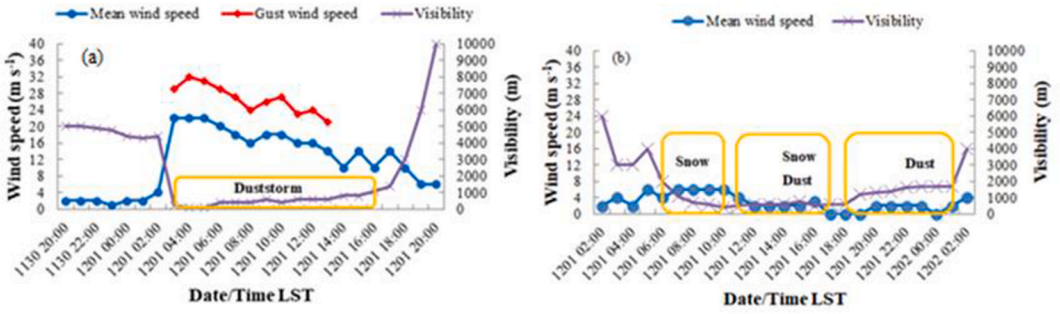

Fig. 8. Hourly surface observations of (gust) wind, visibility (m) and the weather phenomenon (marked inside yellow rectangles) at Karamay (**a**), and Urumqi (**b**) during the episode.

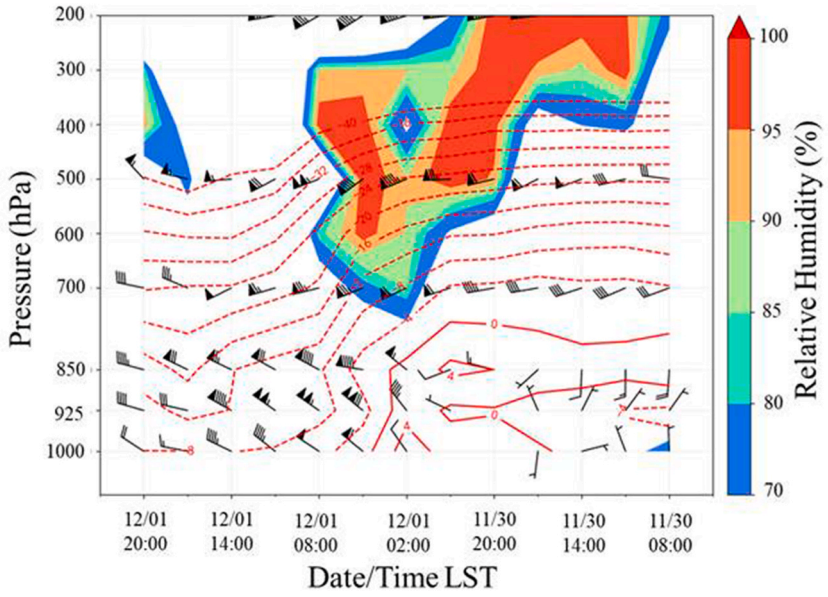

Fig. 9. Vertical profile of wind field (a full barb denotes 4 m s^{-1} and a black pennant denotes 20 m s^{-1}), relative humidity (%) and temperature (°C) over Karamay at 3-h intervals derived from the ECMWF model forecasts initiated at 08:00 LST on 30 November 2018. The dashed red lines indicate the temperatures <0 °C, while the solid red lines indicate the temperatures ≥0 °C.

until 17:00 LST on 1 December, which was favorable for transporting dust to the northeastern areas, such as Mongolia and Siberia, as presented in Figs. 5 and 7.

4. Conclusions

In this paper, the author investigated an unprecedented yellow snow episode occurred in winter in northwest China's Xinjiang Province, where many cases of dust storms are reported in local weather bulletins in spring and early summer every year. What makes this yellow snow episode unique is the large amounts of dust, which tainted the snow yellow, deposited along the transportation corridor in winter, stretching from Karamay to Urumqi.

To identify potential sources and transmission paths of dust, we have analyzed the backward and forward trajectories of air parcels with the HYSPLIT model. From the backward trajectories, it was found that the dust source can be traced back to Kazakhstan. However, Urumqi is not in the path of the forward trajectories starting from Kazakhstan, but in the path of the forward trajectories starting from Karamay. The spatial distribution of dust surface mass concentration obtained from MERRA-2 proved that the dust source in Kazakhstan has no direct links to the dust event occurred in Xinjiang Province. With the separate studies presented here, there is no doubt that the yellow dust originated in Karamay.

The meteorological analysis leads to the conclusion that the upper trough and the cold front traveling through Kazakhstan and China provided favorable meteorological conditions for generating the precipitation and strong winds. Strong surface winds triggered severe dust storm in Karamay and lifted large amounts of dust into the atmosphere. During the following hours, the airborne dusts were

transported to Urumqi rapidly by strong low-level winds. The results indicated that the dust originating from Karamay can affect regions hundreds of kilometers away in a very short time under favorable wind fields.

Despite the wide use of sophisticated Numerical Weather Prediction (NWP) models, accurate and timely forecasts of extreme weather events at long lead times are still out of reach. Traditional methods such as climatological and statistic method always tends to miss extreme weather event. The favorable synoptic situation is not a sufficient predictor of extreme weather event. Under such circumstances, the most important things for forecasters are to pay close attention to abnormal weather event appeared in the upstream regions, make a prompt decision and issue the weather warnings without hesitation when necessary. The lead time may be 1 h to 6 h, but better than nothing. Any delay in acting raises the chance of missing the extreme weather event.

Author contribution statement

Haibo Huang: Conceived and designed the experiments; Wrote the paper.
Yu Wan: Performed the experiments; Analyzed and interpreted the data; Contributed reagents, materials, analysis tools or data.

Data availability statement

Data will be made available on request.

Declaration of competing interest

The authors declare that they have no known competing financial interests or personal relationships that could have appeared to influence the work reported in this paper.

Acknowledgements

We thank two anonymous reviewers for their constructive comments and insightful suggestions. We are also grateful for the help of Qingping Wang with chart making.

References

[1] L.G. Franzén, M. Hjelmroos, P. Kallberg, E. Brorstrom-Lunden, S. Junttoi, A.L. Savolainen, The yellow snow episode of northern Fennoscandia, march 1991—a case study of long-distance transport of soil, pollen and stable organic compounds, Atmos. Environ. 28 (22) (1994) 3587–3604, https://doi.org/10.1016/1352-2310(94)00191-M.
[2] L.G. Franzén, J.O. Mattsson, Martensson, U.T. Nihlén, A. Rapp, Yellow snow over the alps and subarctic from dust storm in africa, March 1991, AMBIO 23 (3) (1994) 233–235, https://doi.org/10.2307/4314206.
[3] L.G. Franzén, M. Hjelmroos, A coloured snow episode on the Swedish west coast - a quantitative and qualitative study of airborne particles, Geogr. Ann. Phys. Geogr. 70 (1988) 235–243, https://doi.org/10.2307/521075.
[4] H.E. Welch, D.C.G. Muir, B.N. Billeck, W.L. Lockhart, G.J. Brunskill, H.J. Kling, M.P. Olson, R.M. Lemoine, Brown snow: a long-range transport event in the Canadian arctic, Environ. Sci. Technol. 25 (2) (1991) 280–286, https://doi.org/10.1021/es00014a010.
[5] J. Lundqvist, K. Bengtsson, The meteorological and pollen analytical study of long transported material from snowfalls in Sweden, Geol. Foren. Stockh. Forh. 92 (1970) 288–301, https://doi.org/10.1080/11035897.1970.9626409.
[6] C.B. Officer, J. Page, Tales of the Earth - paroxysms and perturbations of the blue planet, Earth Sci. Rev. 39 (1995) 127–128, https://doi.org/10.1086/629652.
[7] A. Bucher, J. Dessens, Saharan dust over France and england 6-9 march 1991, JMET (J. Med. Eng. Technol.) 17 (1992) 226–233.
[8] V.P. Shevchenko, V.B. Korobov, A.A.P. Lisitzin, A.S. Aleshinskaya, O.Y. Bogdanova, N.V. Goryunova, First data on the composition of atmospheric dust responsible for yellow snow in northern european Russia in march 2008, Dokl. Earth Sci. 431 (2010) 497–501, https://doi.org/10.1134/S1028334X10040185.
[9] P. Dagsson-Waldhauserova, et al., Snow–dust storm: unique case study from Iceland, march 6–7, 2013, Aeolian. Res. 16 (2015) 69–74. https://doi:10.1016/j.aeolia.2014.11.001.
[10] B. Di Mauro, et al., Mineral dust impact on snow radiative properties in the European Alps combining ground, UAV, and satellite observations, J. Geophys. Res. Atmos. 120 (2015) 6080–6097. https://doi:10.1002/2015JD023287.
[11] S. Lutz, A. Anesio, R. Raiswell, A. Edwards, R.J. Newton, F. Gill, L.G. Benning, The biogeography of red snow microbiomes and their role in melting arctic glaciers, Nat. Commun. 7 (2016), 11968, https://doi.org/10.1038/ncomms11968.
[12] M. Terashima, K. Umezawa, S. Mori, H. Kojima, M. Fukui, Microbial community analysis of colored snow from an alpine snowfield in northern Japan reveals the prevalence of betaproteobacteria with snow algae, Front. Microbiol. 8 (2017) 1481, https://doi.org/10.3389/fmicb.2017.01481.
[13] A.E. Tucker, S.P. Brown, Sampling a gradient of red snow algae bloom density reveals novel connections between microbial communities and environmental features, Sci. Rep. 12 (2022), 10536, https://doi.org/10.1038/s41598-022-13914-7.
[14] C. Persson, H. Rodhe, L.E. De Geer, The Chernobyl accident-a meteorological analysis of how radionuclides reached and were deposited in Sweden, Ambio 16 (1987) 20–31, https://doi.org/10.2307/4313314.
[15] E. Lioubimtseva, G. Henebry, Climate and environmental change in arid Central Asia: impacts, vulnerability, and adaptations, J. Arid Environ. 73 (2009) 963–977, https://doi.org/10.1016/j.jaridenv.2009.04.022.
[16] X. Li, X. Xia, L. Wang, L. Zhao, Z. Feng, The role of foehn in the formation of heavy air pollution events in Urumqi, China, J. Geophys. Res. Atmos. 120 (2015) 5371–5384, https://doi.org/10.1002/2014JD022778.
[17] J.T. Qiu, L. Qiu, H.X. Mu, W.X. Yang, F. Chen, B.K. Yan, Geosites in Karamay city, Xinjiang uygur autonomous region, Northwest China, Geoheritage 11 (2019) 1027–1042, https://doi.org/10.1007/s12371-019-00346-5.
[18] R.R. Draxler, G.D. Hess, An overview of the HYSPLIT_4 modelling system for trajectories, Aust. Meteorol. Mag. 47 (4) (1998) 295–308.
[19] M. Escudero, A.F. Stein, R.R. Draxler, X. Querol, A. Alastuey, S. Castillo, A. Avila, Determination of the contribution of northern Africa dust source areas to PM10 concentrations over the central Iberian Peninsula using the Hybrid Single-Particle Lagrangian Integrated Trajectory model (HYSPLIT) model, J. Geophys. Res. Atmos. 111 (2006), D06210, https://doi.org/10.1029/2005JD006395.
[20] M. Gustafsson, D. Rayner, D. Chen, Extreme rainfall events in southern Sweden: where does the moisture come from? Tellus A. 62 (5) (2010) 605–616, https://doi.org/10.1111/j.1600-0870.2010.00456.x.

[21] R.R. Draxler, P. Ginoux, A.F. Stein, An empirically derived emission algorithm for wind-blown dust, J. Geophys. Res. Atmos. 115 (2010), D16212, https://doi.org/10.1029/2009JD013167.
[22] M. Escudero, A.F. Stein, R.R. Draxler, X. Querol, A. Alastuey, S. Castillo, A. Avila, Source apportionment for African dust outbreaks over the Western Mediterranean using the HYSPLIT model, Atmos. Res. 99 (3–4) (2011) 518–527, https://doi.org/10.1016/j.atmosres.2010.12.002.
[23] Y.Q. Wang, A.F. Stein, R.R. Draxler, J.D. de la Rosa, X.Y. Zhang, Global sand and dust storms in 2008: observation and HYSPLIT model verification, Atmos. Environ. 45 (35) (2011) 6368–6381, https://doi.org/10.1016/j.atmosenv.2011.08.035.
[24] Z.L. Fleming, P.S. Monks, A.J. Manning, Review: untangling the influence of air-mass history in interpreting observed atmospheric composition, Atmos. Res. 104 (105) (2012) 1–39, https://doi.org/10.1016/j.atmosres.2011.09.009.
[25] A.F. Stein, R.R. Draxler, G.D. Rolph, B.J.B. Stunder, M.D. Cohen, F. Ngan, Noaa's hysplit atmospheric transport and dispersion modeling system, Bull. Am. Meteorol. Soc. 96 (12) (2015) 2059–2077, https://doi.org/10.1175/BAMS-D-14-00110.1.
[26] X. Tan, T.Y. Gan, Y.D. Chen, Moisture sources and pathways associated with the spatial variability of seasonal extreme precipitation over Canada, Clim. Dynam. 50 (1–2) (2018) 629–640, https://doi.org/10.1007/s00382-017-3630-0.
[27] C.A. Álvarez, J.N. Carbajal, L.F. Pineda-Martínez, J. Tuxpan, D.E. Flores, Dust deposition on the gulf of California caused by santa ana winds, Atmosphere 11 (3) (2020) 275, https://doi.org/10.3390/atmos11030275.
[28] P. Broomandi, F. Karaca, M. Guney, A. Fathian, X.Y. Geng, J.R. Kim, Destinations frequently impacted by dust storms originating from Southwest Iran, Atmos. Res. 248 (1) (2020), 105264, https://doi.org/10.1016/j.atmosres.2020.105264.
[29] O.D. Santos, L. Hoinaski, Incorporating gridded concentration data in air pollution back trajectories analysis for source identification, Atmos. Res. 263 (2021), 105820, https://doi.org/10.1016/j.atmosres.2021.105820.
[30] Y.Q. Wang, X.Y. Zhang, R.R. Draxler, TrajStat: GIS-based software that uses various trajectory statistical analysis methods to identify potential sources from long-term air pollution measurement data, Environ. Model. Software 24 (2009) 938–939, https://doi.org/10.1016/j.envsoft.2009.01.004.
[31] F.L. Wang, L. Y, Sun, Y. Tao, Y.T. Guo, Z.Q. Li, X.G. Zhao, S. Zhou, Pollution characteristics in a dusty season based on highly time-resolved online measurements in northwest China, Sci. Total Environ. 650 (2019) 2545–2558, https://doi.org/10.1016/j.scitotenv.2018.09.382.
[32] S. Khanal, R.P. Pokhrel, B. Pokharel, S. Becker, B. Giri, L. Adhikari, M.D. LaPlante, An episode of transboundary air pollution in the central Himalayas during agricultural residue burning season in North India, Atmos, Pollut. Res. 13 (1) (2022), 101270, https://doi.org/10.1016/j.apr.2021.101270.
[33] M.M. Rienecker, et al., MERRA: NASA's Modern-Era Retrospective analysis for research and applications, J. Clim. 24 (2011) 3624–3648, https://doi.org/10.1175/JCLI-D-11-00015.1.
[34] R. Gelaro, W. McCarty, M.J. Suárez, R. Todling, A. Molod, L. Takacs, The modern-era retrospective analysis for research and applications, version 2 (MERRA-2), J. Clim. 30 (14) (2017) 5419–5454, https://doi.org/10.1175/JCLI-D-16-0758.1.
[35] C.A. Randles, A.M. da Silva, V. Buchard, The MERRA-2 aerosol reanalysis, 1980 onward. Part I: system description and data assimilation evaluation, J. Clim. 30 (17) (2017) 6823–6850, https://doi.org/10.1175/JCLI-D-16-0609.1.
[36] J. Acker, R. Soebiyanto, R. Kiang, S. Kempler, Geo-information use of the NASA giovanni data system for geospatial public health research: example of weather-influenza connection, ISPRS Int. J. Geo-Inf. 3 (4) (2014) 1372–1386, https://doi.org/10.3390/ijgi3041372.
[37] W.J. Steenburgh, J.D. Massey, T.H. Painter, Episodic dust events of Utah's wasatch front and adjoining region, J. Appl. Meteorol. Climatol. 51 (9) (2012) 1654–1669, https://doi.org/10.1175/JAMC-D-12-07.1.
[38] H.S. Xie, L.D. Wu, W. Xie, Q. Lin, M. Liu, Y.J. Lin, Improving ECMWF short-term intensive rainfall forecasts using generative adversarial nets and deep belief networks, Atmos. Res. 249 (2020), 105281, https://doi.org/10.1016/j.atmosres.2020.105281.
[39] X.M. Wei, X.G. Sun, Z.M. Liang, Linking ECMWF 2 m temperature forecast errors with upper-level circulation situation: a case-study for China, Atmosphere 12 (2021) 725, https://doi.org/10.3390/atmos12060725.
[40] W.H. Qian, L.S. Quan, Y.S. Shi, Variations of the dust storm in China and its climatic control, J. Clim. 15 (10) (2002) 1216–1229, https://doi.org/10.1175/1520-0442(2002)015<1216:votdsi>2.0.co, 2.
[41] J. Yang, et al., Temporal and spatial variations of sandstorm and the related meteorological influences over northern China from 2000 to 2019, Acta Sci. Circumstantiae 41 (8) (2021) 2966–2975 (in Chinese).
[42] I. Uno, K. Eguchi, K. Yumimoto, T. Takemura, A. Shimizu, M. Uematsu, Asian dust transported one full circuit around the globe, Nat. Geosci. 2 (8) (2009) 557–560, https://doi.org/10.1038/ngeo583.
[43] Y. Yan, Y. Sun, L. Ma, X. Long, A multidisciplinary approach to trace asian dust storms from source to sink, Atmos. Environ. 105 (2015) 43–52, https://doi.org/10.1016/j.atmosenv.2015.01.039.
[44] Q.Y. Guan, F.C. Li, L.Q. Yang, R. Zhao, Y.Y. Yang, H.P. Luo, Spatial-temporal variations and mineral dust fractions in particulate matter mass concentrations in an urban area of northwestern China, J. Environ. Manag. 222 (2018) 95–103, https://doi.org/10.1016/j.jenvman.2018.05.064.
[45] A.S. Goudie, N.J. Middleton, Saharan dust storms: nature and consequences, Earth Sci. Rev. 56 (1–4) (2001) 179–204, https://doi.org/10.1016/S0012-8252(01)00067-8.
[46] R.R. Draxler, D.A. Gillette, J.S. Kirkpatrick, J. Heller J, Estimating PM10 air concentrations from dust storms in Iraq, Kuwait, and Saudi Arabia, Atmos, 2001, Environ. Times 35 (25) (2001) 4315–4330, https://doi.org/10.1016/S1352-2310(01)00159-5.
[47] A. Stohl, S. Eckhardt, C. Forster, P. James, N. Spichtinger, P. Seibert, A replacement for simple back trajectory calculations in the interpretation of atmospheric trace substance measurements, Atmos. Environ. 36 (29) (2002) 4635–4648, https://doi.org/10.1016/S1352-2310(02)00416-8.
[48] J.C. Lin, C. Gerbig, S.C. Wofsy, A near-field tool for simulating the upstream influence of atmospheric observations: the stochastic time-inverted Lagrangian transport (STILT) model, J. Geophys. Res. Atmos. 108 (2003) D16, https://doi.org/10.1029/2002JD003161.
[49] J.Q. Zhao, X.Y. Ma, S.Q. Wu, T. Sha, Dust emission and transport in Northwest China: WRF-Chem simulation and comparisons with multi-sensor observations, Atmos. Res. 241 (2020), 104978, https://doi.org/10.1016/j.atmosres.2020.104978.
[50] B.H. Alharbi, A. Maghrabi, N. Tapper, The march 2009 dust event in Saudi arabia precursor and supportive environment, Bull. Am. Meteorol. Soc. 94 (4) (2013) 515–528, https://doi.org/10.1175/BAMS-D-11-00118.